Organizing combinatorial transcription factor recruitment at cis -regulatory modules

Julie Dubois Dubois-Chevalier, Parisa Mazrooei, Mathieu Lupien, Bart Staels, Philippe Lefebvre, Jérôme Eeckhoute

▶ **To cite this version:**

Julie Dubois Dubois-Chevalier, Parisa Mazrooei, Mathieu Lupien, Bart Staels, Philippe Lefebvre, et al.. Organizing combinatorial transcription factor recruitment at cis -regulatory modules. Transcription, 2018, 9 (4), pp.233-239. 10.1080/21541264.2017.1394424 . inserm-02153895

HAL Id: inserm-02153895

https://inserm.hal.science/inserm-02153895v1

Submitted on 12 Jun 2019

HAL is a multi-disciplinary open access archive for the deposit and dissemination of scientific research documents, whether they are published or not. The documents may come from teaching and research institutions in France or abroad, or from public or private research centers.

L'archive ouverte pluridisciplinaire **HAL**, est destinée au dépôt et à la diffusion de documents scientifiques de niveau recherche, publiés ou non, émanant des établissements d'enseignement et de recherche français ou étrangers, des laboratoires publics ou privés.

Organizing combinatorial transcription factor recruitment at *cis*-regulatory modules

Julie Dubois-Chevalier [1], Parisa Mazrooei [2], Mathieu Lupien [2], Bart Staels [1], Philippe Lefebvre [1,§], Jérôme Eeckhoute [1,§,*]

[1] Univ. Lille, Inserm, CHU Lille, Institut Pasteur de Lille, U1011- EGID, F-59000 Lille, France

[2] The Princess Margaret Cancer Centre, University Health Network, Department of Medical Biophysics, University of Toronto, Toronto, ON M5G 1L7, Canada

[§] Joint senior authors

[*] Corresponding author:

Dr. Jérôme Eeckhoute

INSERM UMR 1011-Bâtiment J&K

Université Lille 2; Faculté de Médecine de Lille-Pôle Recherche

Boulevard du Professeur Leclerc

59045 Lille cedex

France

Tel: 33(0)3 20 97 42 20 / Fax: 33(0)3 20 97 42 01

E-mail: jerome.eeckhoute@inserm.fr

Keywords

Chromatin binding, *cis*-regulatory modules, DNA recognition elements, functional genomics, liver, transcription factors, *trans*-regulatory modules, single nucleotide variants

Abstract

Gene transcriptional regulation relies on *cis*-regulatory DNA modules (CRMs), which serve as nexus sites for integration of multiple transcription factor (TF) activities. Here, we provide evidence and discuss recent literature indicating that TF recruitment to CRMs is organized into combinations of *trans*-regulatory protein modules (TRMs). We propose that TRMs are functional entities composed of TFs displaying the most highly interdependent chromatin binding which are, in addition, able to modulate their recruitment to CRMs through inter-TRM effects. These findings shed light on the architectural organization of TF recruitment encoded by their recognition motifs within CRMs.

Gene expression regulation involves combinatorial recruitment of multiple transcription factors (TFs) organized into modules at transcriptional regulatory regions

Transcriptional regulation is one of the main control steps involved in specifying appropriate gene expression. Cells rely on an array of transcription factors (TFs), which total several hundreds in higher Eukaryotes [1], to finely tune gene expression. This is achieved through concomitant regulation of a given gene by multiple TFs, which combine activities at *cis*-regulatory modules (CRMs) including promoters and enhancers [2]. Combinatorial regulation of gene expression by multiple TFs allows cells to handle the challenging task of controlling their transcriptome with specificity, robustness and adaptability to environmental signals. For instance, the concentration of TF binding sites or their DNA recognition motifs [hereafter called response elements (REs)] is highly predictive of strong enhancer activity [3]. In this context, understanding how recruitment and activities of multiple TFs are functionally orchestrated at CRMs constitutes fundamental questions in the field of transcriptional regulation.

It has been well established, in different biological systems and using a compendium of various technical approaches, that TF co-recruitment to CRMs often does not lead to a mere additive effect but actually implies functional interferences between TF activities. These interferences can be positive or negative and are exerted though direct or indirect mechanisms [4,5]. Direct effects are mediated through TF-TF interactions, which can modulate TF functions (cofactor recruitment, DNA binding) through steric hindrance or induced conformational changes [6]. Competition for REs has also been reported [7]. Indirect functional interference between TFs often involves modulation of their binding to CRMs through chromatin-based mechanisms [8,9]. Indeed, by remodelling the local chromatin structure through nucleosome positioning and/or epigenetic modifications (of DNA and/or histones), a given TF can indirectly modulate recruitment to CRMs of another TF. In this context, hierarchical

recruitment of TF to chromatin has been reported, where pioneer TFs bind to and remodel condensed chromatin to allow subsequent binding of subordinate TFs [10,11]. In line with TF interdependent chromatin binding, it has been reported that allelic imbalance in occupancy or changes in a given TF genomic recruitment across evolution can not be entirely explained by genetic variation occurring directly in its RE [12,13].

Understanding how RE organization within CRMs translates into concerted TF recruitment has relevance not only for our basic knowledge of CRM evolution and transcriptional regulatory activities, but is also directly relevant to human diseases. Indeed, changes in TF binding to chromatin and CRM activities trigger abnormal transcriptomes such as those linked to enhancer reprogramming in cancer [14]. Moreover, many single nucleotide variants (SNVs) which modulate traits or disease occurrence have been shown or predicted to impact REs, TF DNA binding domains and/or TF chromatin binding [15–17].

Using mouse liver gene transcriptional regulation as a model system, we have recently described that different subsets of TFs (and cofactors) show preferential and interdependent co-binding to CRMs, thereby defining *trans*-regulatory modules (TRMs) [18]. Modular combinatorial binding of TFs has also been inferred from hundreds of TF binding data from the K562 cell-line [19]. In the liver, in addition to a core set of TFs broadly bound to liver CRMs, we found that liver-specific gene transcriptional regulation involves the combinatorial recruitment of 3 types of TRMs comprising a promoter TRM, a TRM specifically and broadly controlling hepatic functions and a facultative circadian TRM (Fig.1A). We also confirmed that the presence of REs directly recognized by TFs from a given TRM was, in most instances, instructive for its presence at CRMs.

Interdependent chromatin recruitment of TFs within liver TRMs

In our study, organization of TF chromatin recruitment into combinations of TRMs was further indicated by results from intra-genomic replicate (IGR) analyses [20,21]. The IGR tool predicts the impact of SNVs on TF chromatin binding by comparing the average TF ChIP-seq signal intensity across the genomic loci that contains the reference or the variant allele of each SNV (within underlying sequences of 7-mers) [20,21]. This allowed to define that SNVs concomitantly and preferentially impact chromatin binding of TFs comprised within the same TRM [18]. To define which REs were impacted by the analyzed SNVs, we used PERFECTOS-APE [22]. This tool first identified REs overlapping our SNVs of interest and then predicted how these SNVs may alter TF binding affinity to these overlapping REs. The obtained results were then used to define how changes in RE affinity correlate with changes in TF binding to chromatin previously defined by IGR (Fig.1B). Hierarchical clustering of the data identified clusters of REs positively correlated with clusters of TFs, which we define as blocks (Fig.1C). For instance, blocks linking TFs from the promoter TRM to E2F/EGR/ETS motifs, the TRM specifically controlling hepatic functions to FOX/CEBP/PAR-bZIP/Homeobox (HNF6) motifs and the circadian TRM to E-boxes were highlighted by these analyses (framed in Fig.1C; see Table S1 for a full list of motifs). These analyses predicted that, in addition to being required for recruitment of their cognate TFs, individual REs are also often important for the co-recruitment of additional TFs within TRMs. This suggests a lack of strong hierarchy in TF recruitment within TRMs where many individual TFs can modulate recruitment of the broad set of TFs these modules comprise. An additional block corresponding to many, but not all, nuclear receptors (NRs) and their REs was also identified in Fig.1C. This NR block comprised several NRs from the core set of TFs which are essential regulators of liver functions (RXRA, HNF4A, PPARA, NR1D2/REV-ERB beta). Of note, some other NRs showed an opposite correlation between predicted SNV-induced changes in NR RE affinity and their chromatin binding (NR1H3/LXR alpha and NR1H4/FXR). These

results are in line with a previous study showing that PPARA and NR1H3/LXR alpha bind to overlapping sites in a mutually exclusive manner in the mouse liver [7]. This also further indicates extensive NR crosstalk at shared liver CRMs where common REs fine tune chromatin binding of many NR family members. NR5A2/LRH-1 and RARA, which displayed poor correlation with NR RE, may be recruited to promoters through other means such as tethering [18].

Liver TRMs show different levels of mutual interference in chromatin recruitment

A lack of correlation (Fig.1C) does not however imply that SNVs modulating RE affinity do not impact on TF chromatin binding because milder effects may be more difficult to call with statistical significance or context-specific effects could lead to divergent consequences on TF binding at different CRMs. Therefore, we next compiled SNVs modulating RE affinity from each cluster (1 to 11) and monitored the fraction predicted to modulate binding of each TF. This revealed that most clusters of motifs from Fig.1C were predicted to modulate recruitment of TFs outside from the TRM comprising their cognate TF (Fig.1D). For example, SNVs modulating NR RE affinity (clusters 10-11) broadly modulate chromatin binding of other TFs while NR chromatin binding is in return affected by changes in RE affinity from most other clusters (Fig.1D). The lack of correlation (Fig.1C) is most probably to be ascribed to weaker and more complex indirect effects when SNVs influence chromatin binding of TFs from a different TRM. Importantly, reciprocal influences are not always symmetrical and are even absent in some instances. For example, SNVs in motifs from cluster 1 modulate binding of TFs defining the promoter TRM (RARA, NR5A2, GABPA, E2F4), but not that of TFs from the liver-specific functions control TRM (HNF1A, FOXA2, RORA, NFIL3, FOXA1), while the opposite was true for SNVs in motifs from

clusters 6 to 9 (Fig.1D). This suggests that recruitment of these 2 TRMs is functionally independent at liver CRMs.

Discussion and perspectives

Altogether, the data presented in [18] and herein point to a hierarchical model of TF interdependent chromatin recruitment where the most highly interdependent TFs define TRMs which can secondarily impact on each other (Fig.2).

This suggests that TRMs consist of sets of TFs whose chromatin binding is influenced as a bulk by individual REs. Indeed, while not all show the same importance, our data indicate a broad array of REs/TFs is able to influence a given TRM recruitment. A hierarchy with a few specific REs/TFs, such as pioneer TFs, controlling recruitment of other TFs from the same TRM could not be clearly identified. Recent studies have indicated that pioneer TF chromatin binding can be modulated by surrogate TFs [23,24]. For instance, during pluripotency reprogramming by Oct4, Sox2, Klf4, and c-Myc (O,S,K and M), OSK act as pioneer TFs for M which, in return, stabilizes OSK chromatin recruitment [23]. Hence, the hierarchy of TF recruitment enabling CRM activation during cell differentiation or reprogramming is most probably largely lost once cells have acquired a new stable state where CRM activation is maintained through acquired additional cooperative TF binding (Fig.2).

Beyond intra-TRM regulation of TF chromatin binding, how TRMs mutually influence their recruitment to CRMs (inter-TRM modulations) (Fig.2) will be a challenging and important question to tackle. This may require to better define the RE grammar which governs their arrangements at CRMs and how this specifies TRM recruitment and crosstalk. Going deeper into understanding CRM organization will undoubtedly benefit from a better knowledge of the actual diversity of REs involved in TF recruitment [5]. Indeed, many TF REs are unknown and recent studies suggest that the spectrum of RE recognized by a given TF

may extend well beyond what has been defined so far [25–27]. In addition, within the nucleus, CRMs co-ordinately regulating common gene(s) are found in close proximity, involving for example long-range contacts between promoters and enhancers [28]. In this context, how TRMs at a given CRM influence TRM binding at another functionally interconnected CRM constitutes another important question. Recent advances in genomic editing technologies including those using CRISPR/Cas9 as well as novel approaches allowing for analysis of the proteome bound to single CRM [29] will undoubtedly contribute to better define how TRM recruitment is orchestrated at CRMs in the near future.

In summary, we envision TRMs as entities allowing for the integration of activities of highly interdependent and interconnected TFs, which bring specific transcriptional regulatory inputs secondarily integrated altogether to provide genes with coordinated transcriptional regulatory signals. In this context, it will be instrumental to define how the identified TF interdependent binding within and across TRM evolves in different (patho)physiological conditions. Finally, and most importantly, this knowledge will need to be leveraged to better understand how TF interdependent chromatin binding functionally translates into transcriptional regulatory outputs [4,18].

Materials and Methods

Analyses were performed using CRM involved in liver-specific gene regulation which we have previously identified, i.e. CRM^{G} from [18].

The intra-genomic replicate (IGR) tool [20,21] was used to predict the impact of single nucleotide variants (SNVs) found within CRM^{G} as described in [18].

PERFECTOS-APE [22] version 2.0.3 was used with the HOCOMOCOv10 mononucleotide PWMs and their pre-computed thresholds [30] to define how these SNVs impact on transcription factor response elements (REs) with parameters.

Fold changes provided by IGR and PERFECTOS-APE were retrieved when significant effects (FDR<0.05) were found. Fold changes were set to 0 when statistical significance was not reached.

Correlation between IGR and PERFECTOS-APE data was performed using the "cor" function of the R package "stat" [31].

Heatmaps and hierarchical clusterings were obtained using the heatmap.2 function of the R package "gplots" [32] using euclidean distance and aggregation method "ward.D2"

Similar motifs were clustered based on matrix similarities using RSAT matrix-clustering with parameters : hclust_method = average, metric_build_tree = NCor, calc= sum, lth w = 5, lth cor = 0.6, lth NCor = 0.4 and quick = true [33]

Disclosure of potential conflicts of interest

The authors have no potential conflicts of interest to disclose.

Funding

This work was supported by grants from the Fondation pour la Recherche Médicale (Equipe labellisée, DEQ20150331724), "European Genomic Institute for Diabetes" (E.G.I.D., ANR-10-LABX-46) and European Commission. B.S. is supported by the European Research Council (ERC Grant Immunobile, contract 694717).

Legend to figures

Figure 1. Definition of TF interdependent binding to CRMs through comparison of SNV-induced changes in RE affinity and TF chromatin binding

A) Summary of the main conclusions drawn from [18] showing that TFs (and cofactors) bind to mouse liver CRMs as TRMs consisting of factors with preferential interdependent co-

recruitment. **B)** Schematic representation of the strategy used to compare SNVs-mediated changes in RE affinity and TF chromatin binding. Impact of SNVs on REs was defined using PERFECTOS-APE [22] while their impact on TF chromatin binding was predicted through mining liver ChIP-seq data using IGR [20,21]. Details are provided in the Materials and Methods section. **C)** Correlations between SNV-induced changes in RE affinity and TF chromatin binding were defined using cor function of R package "stat" as detailed in the Materials and Methods section. The heatmap shows how changes in affinity of individual REs correlate with that in TF chromatin binding. The main RE families from clusters 1 to 11 are indicated at the bottom (see Table S1 for the full list of REs contained in each cluster). TFs and cofactors are colored according to Fig.1A. Hierarchical clustering trees are shown on top and on the left. **D)** SNVs were assigned the best predicted impacted RE by PERFECTOS-APE, which were then used to define the fraction of REs from a given cluster which had been predicted to impact TF/cofactor chromatin binding by IGR. The heatmap shows the percent of SNVs impacting motifs comprised within clusters 1 to 11 (defined in Fig.1C) which were concomitantly predicted to impact a given TF/cofactor chromatin binding. Hierarchical clustering trees are shown on top and on the left.

Figure 2. Proposed model of combinatorial TF recruitment organization at liver CRMs.

See text for details.

References

1. Zhang H-M, Chen H, Liu W, Liu H, Gong J, Wang H, Guo A-Y. AnimalTFDB: a comprehensive animal transcription factor database. Nucleic Acids Res 2012; 40:D144–9.

2. Gerstein MB, Kundaje A, Hariharan M, Landt SG, Yan K-K, Cheng C, Mu XJ, Khurana E, Rozowsky J, Alexander R, et al. Architecture of the human regulatory network derived from ENCODE data. Nature 2012; 489:91–100.

3. Santiago-Algarra D, Dao LTM, Pradel L, España A, Spicuglia S. Recent advances in high-throughput approaches to dissect enhancer function. F1000Research 2017; 6:939.

4. Grossman SR, Zhang X, Wang L, Engreitz J, Melnikov A, Rogov P, Tewhey R, Isakova A, Deplancke B, Bernstein BE, et al. Systematic dissection of genomic features determining transcription factor binding and enhancer function. Proc Natl Acad Sci U S A 2017; 114:E1291–300.

5. Weingarten-Gabbay S, Segal E. The grammar of transcriptional regulation. Hum Genet 2014; 133:701–11.

6. Weikum ER, Knuesel MT, Ortlund EA, Yamamoto KR. Glucocorticoid receptor control of transcription: precision and plasticity via allostery. Nat Rev Mol Cell Biol 2017; 18:159–74.

7. Boergesen M, Pedersen TÅ, Gross B, van Heeringen SJ, Hagenbeek D, Bindesbøll C, Caron S, Lalloyer F, Steffensen KR, Nebb HI, et al. Genome-wide profiling of liver X receptor, retinoid X receptor, and peroxisome proliferator-activated receptor α in mouse liver reveals extensive sharing of binding sites. Mol Cell Biol 2012; 32:852–67.

8. Heinz S, Romanoski CE, Benner C, Allison KA, Kaikkonen MU, Orozco LD, Glass CK. Effect of natural genetic variation on enhancer selection and function. Nature 2013; 503:487–92.

9. Pham T-H, Minderjahn J, Schmidl C, Hoffmeister H, Schmidhofer S, Chen W, Längst G, Benner C, Rehli M. Mechanisms of in vivo binding site selection of the hematopoietic master transcription factor PU.1. Nucleic Acids Res 2013; 41:6391–402.

10. Magnani L, Eeckhoute J, Lupien M. Pioneer factors: directing transcriptional regulators within the chromatin environment. Trends Genet 2011; 27:465–74.

11. Zaret KS, Carroll JS. Pioneer transcription factors: establishing competence for gene expression. Genes Dev 2011; 25:2227–41.

12. Reddy TE, Gertz J, Pauli F, Kucera KS, Varley KE, Newberry KM, Marinov GK, Mortazavi A, Williams BA, Song L, et al. Effects of sequence variation on differential allelic transcription factor occupancy and gene expression. Genome Res 2012; 22:860–9.

13. Stefflova K, Thybert D, Wilson MD, Streeter I, Aleksic J, Karagianni P, Brazma A, Adams DJ, Talianidis I, Marioni JC, et al. Cooperativity and rapid evolution of cobound transcription factors in closely related mammals. Cell 2013; 154:530–40.

14. Roe J-S, Hwang C-I, Somerville TDD, Milazzo JP, Lee EJ, Da Silva B, Maiorino L, Tiriac H, Young CM, Miyabayashi K, et al. Enhancer Reprogramming Promotes Pancreatic Cancer Metastasis. Cell 2017; 170:875–888.e20.

15. Barrera LA, Vedenko A, Kurland JV, Rogers JM, Gisselbrecht SS, Rossin EJ, Woodard J, Mariani L, Kock KH, Inukai S, et al. Survey of variation in human transcription factors reveals prevalent DNA binding changes. Science 2016; 351:1450–4.

16. Maurano MT, Haugen E, Sandstrom R, Vierstra J, Shafer A, Kaul R, Stamatoyannopoulos JA. Large-scale identification of sequence variants influencing human transcription factor occupancy in vivo. Nat Genet 2015; 47:1393–401.

17. Zhou S, Treloar AE, Lupien M. Emergence of the Noncoding Cancer Genome: A Target of Genetic and Epigenetic Alterations. Cancer Discov 2016; 6:1215–29.

18. Dubois-Chevalier J, Dubois V, Dehondt H, Mazrooei P, Mazuy C, Sérandour AA, Gheeraert C, Guillaume P, Baugé E, Derudas B, et al. The logic of transcriptional regulator recruitment architecture at cis-regulatory modules controlling liver functions. Genome Res 2017; 27:985–96.

19. Guo Y, Gifford DK. Modular combinatorial binding among human trans-acting factors reveals direct and indirect factor binding. BMC Genomics 2017; 18:45.

20. Cowper-Sal lari R, Zhang X, Wright JB, Bailey SD, Cole MD, Eeckhoute J, Moore JH, Lupien M. Breast cancer risk-associated SNPs modulate the affinity of chromatin for FOXA1 and alter gene expression. Nat Genet 2012; 44:1191–8.

21. Bailey SD, Desai K, Kron KJ, Mazrooei P, Sinnott-Armstrong NA, Treloar AE, Dowar M, Thu KL, Cescon DW, Silvester J, et al. Noncoding somatic and inherited single-nucleotide variants converge to promote ESR1 expression in breast cancer. Nat Genet 2016; 48:1260–6.

22. Vorontsov IE, Kulakovskiy IV, Khimulya G, Nikolaeva DD, Makeev VJ. PERFECTOS-APE - Predicting Regulatory Functional Effect of SNPs by Approximate P-value Estimation [Internet]. 2017 [cited 2017 Aug 10]. page 102–8.Available from: http://www.scitepress.org/DigitalLibrary/Link.aspx?doi=10.5220/0005189301020108

23. Soufi A, Donahue G, Zaret KS. Facilitators and impediments of the pluripotency reprogramming factors' initial engagement with the genome. Cell 2012; 151:994–1004.

24. Swinstead EE, Miranda TB, Paakinaho V, Baek S, Goldstein I, Hawkins M, Karpova TS, Ball D, Mazza D, Lavis LD, et al. Steroid Receptors Reprogram FoxA1 Occupancy through Dynamic Chromatin Transitions. Cell 2016; 165:593–605.

25. Isakova A, Groux R, Imbeault M, Rainer P, Alpern D, Dainese R, Ambrosini G, Trono D, Bucher P, Deplancke B. SMiLE-seq identifies binding motifs of single and dimeric transcription factors. Nat Methods 2017; 14:316–22.

26. Jolma A, Yin Y, Nitta K, Dave K, Popov A, Taipale M, Enge M, Kivioja T, Morgunova E, Taipale J. DNA-dependent formation of transcription factor pairs alters their binding specificity. Nature 2015; 527:384–8.

27. Neph S, Vierstra J, Stergachis A, Reynolds A, Haugen E, Vernot B, Thurman R, John S, Sandstrom R, Johnson A, et al. An expansive human regulatory lexicon encoded in transcription factor footprints. Nature 2012; 489:83–90.

28. de Laat W, Duboule D. Topology of mammalian developmental enhancers and their regulatory landscapes. Nature 2013; 502:499–506.

29. Liu X, Zhang Y, Chen Y, Li M, Zhou F, Li K, Cao H, Ni M, Liu Y, Gu Z, et al. In Situ Capture of Chromatin Interactions by Biotinylated dCas9. Cell 2017; 170:1028–1043.e19.

30. Kulakovskiy IV, Vorontsov IE, Yevshin IS, Soboleva AV, Kasianov AS, Ashoor H, Ba-Alawi W, Bajic VB, Medvedeva YA, Kolpakov FA, et al. HOCOMOCO: expansion and enhancement of the collection of transcription factor binding sites models. Nucleic Acids Res 2016; 44:D116-125.

31. R Core Team. R: A language and environment for statistical computing. R Found Stat Comput [Internet] 2015; Available from: http://www.R-project.org.

32. Warnes G, Bolker B, Bonebakker L, Gentleman R, Liaw W, Lumley T, Maechler M, Magnusson A, Moeller S, Schwartz M, et al. gplots: Various R Programming Tools for Plotting Data. R package version 3.0.1. 2016; Available from: https://CRAN.R-project.org/package=gplots

33. Castro-Mondragon JA, Jaeger S, Thieffry D, Thomas-Chollier M, van Helden J. RSAT matrix-clustering: dynamic exploration and redundancy reduction of transcription factor binding motif collections. Nucleic Acids Res 2017; 45:e119.

Fig.1

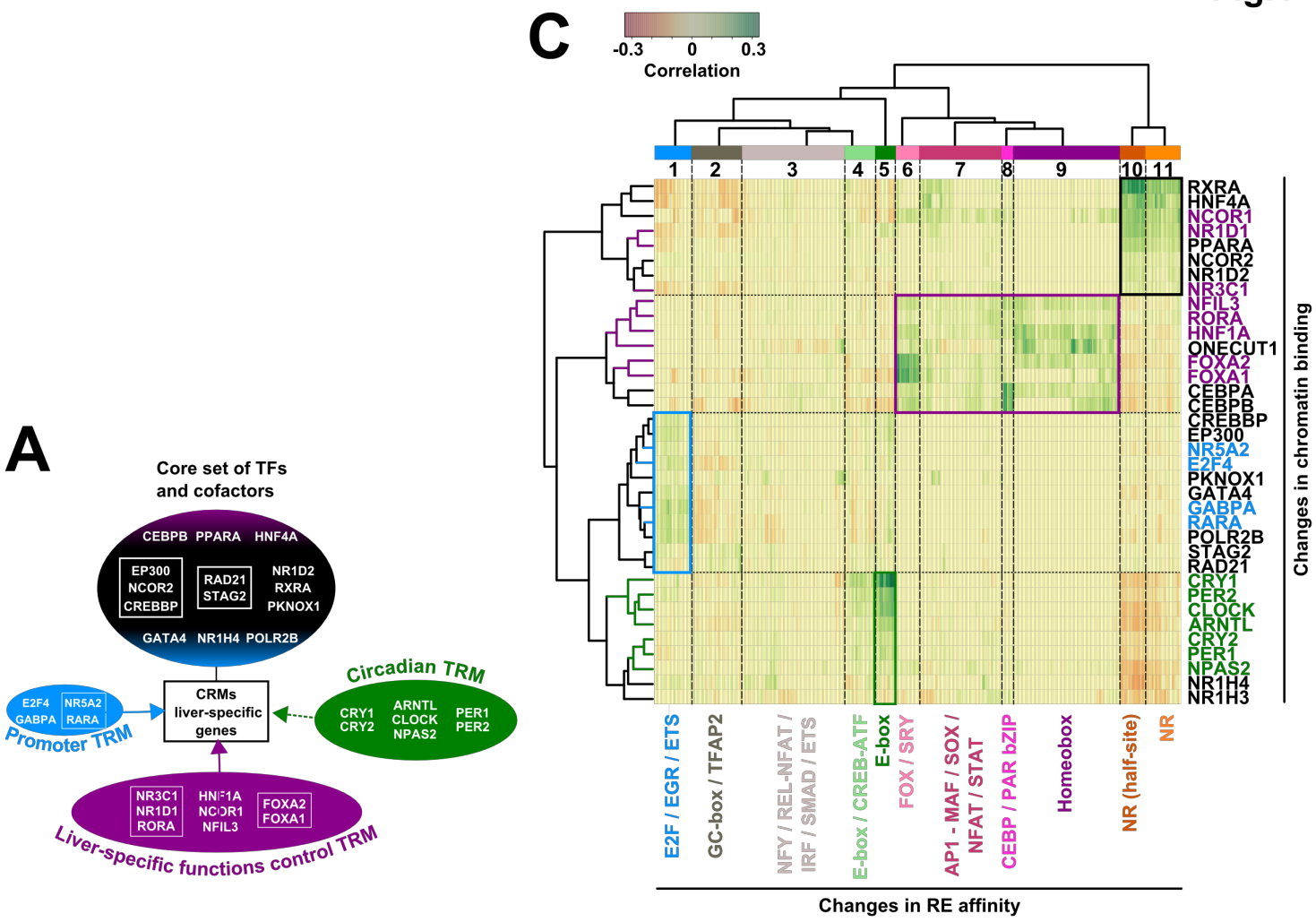
A
Core set of TFs and cofactors
CEBPB PPARA HNF4A
EP300 NCOR2 CREBBP
RAD21 STAG2
NR1D2 RXRA PKNOX1
GATA4 NR1H4 POLR2B
CRMs liver-specific genes
E2F4 NR5A2 GABPA RARA
Promoter TRM
Circadian TRM
CRY1 CRY2 ARNTL CLOCK NPAS2 PER1 PER2
NR3C1 NR1D1 RORA HNF1A NCOR1 NFIL3 FOXA2 FOXA1
Liver-specific functions control TRM
C
-0.3 0 0.3
Correlation
1 2 3 4 5 6 7 8 9 10 11
RXRA HNF4A NCOR1 NR1D1 PPARA NCOR2 NR1D2 NR3C1 NFIL3 RORA HNF1A ONECUT1 FOXA2 FOXA1 CEBPA CEBPB CREBBP EP300 NR5A2 E2F4 PKNOX1 GATA4 GABPA RARA POLR2B STAG2 RAD21 CRY1 PER2 CLOCK ARNTL CRY2 PER1 NPAS2 NR1H4 NR1H3
Changes in chromatin binding
E2F / EGR / ETS
GC-box / TFAP2
NFY / REL-NFAT / IRF / SMAD / ETS
E-box / CREB-ATF
E-box
FOX / SRY
AP1 - MAF / SOX / NFAT / STAT
CEBP / PAR bZIP
Homeobox
NR (half-site)
NR
Changes in RE affinity
B
+/- TF chromatin binding
IGR
SNV
PERFECTOS-APE
+/- RE affinity
Circadian TFs
Liver-specific functions control TFs
Core TFs
Promoter TFs
T/A
D
% of SNVs modulating chromatin recruitment
1 3 2 4 5 10 11 8 7 6 9
HNF4A RXRA NR3C1 NR1D1 PPARA NR1D2 NR1H3 CLOCK PER1 CRY1 CRY2 NPAS2 ARNTL HNF1A FOXA2 ONECUT1 CEBPA RORA NFIL3 FOXA1 CEBPB NCOR1 STAG2 RAD21 PKNOX1 NCOR2 PER2 CREBBP EP300 GATA4 NR1H4 POLR2B RARA NR5A2 GABPA E2F4
E2F / EGR / ETS
NFY / REL-NFAT / IRF / SMAD / ETS
GC-box / TFAP2
E-box / CREB-ATF
E-box
NR (half-site)
NR
CEBP / PAR bZIP
AP1 - MAF / SOX / NFAT / STAT
FOX / SRY
Homeobox

Fig.2

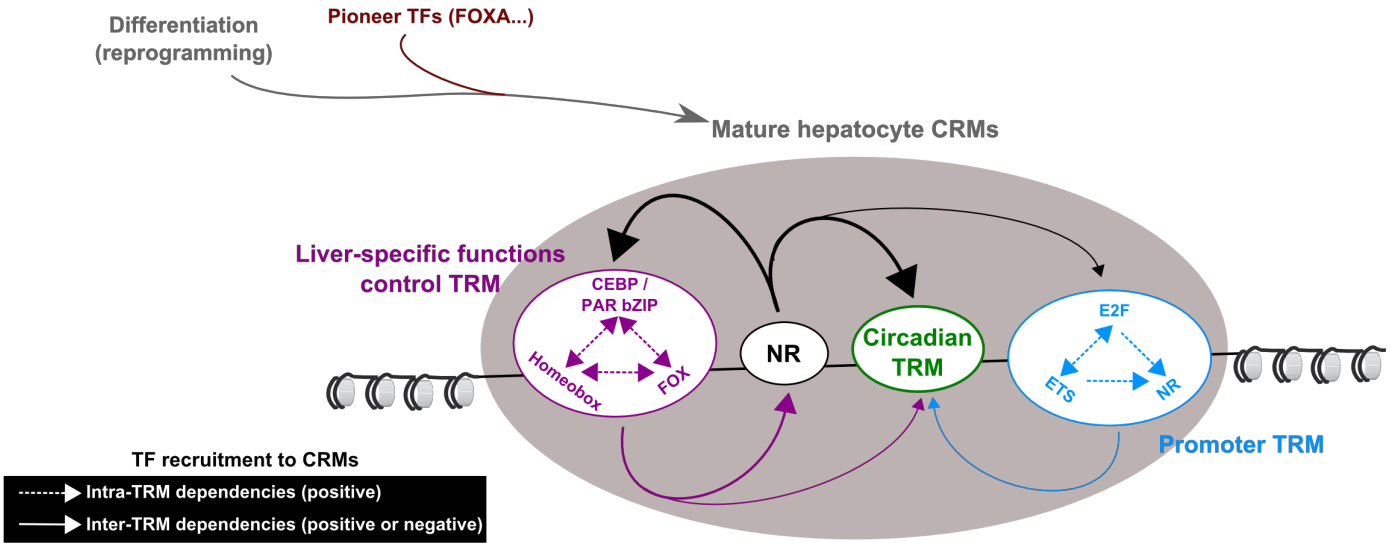
Differentiation
(reprogramming)
Pioneer TFs (FOXA...)
Mature hepatocyte CRMs
Liver-specific functions
control TRM
CEBP /
PAR bZIP
Homeobox
FOX
NR
Circadian
TRM
E2F
ETS
NR
Promoter TRM
TF recruitment to CRMs
Intra-TRM dependencies (positive)
Inter-TRM dependencies (positive or negative)

Heatmap cluster 1

RSAT matrix-clustering	cluster_1	Collection_1_m27_SP2_MOUSE.H10MO.C,Collection_1_m30_WT1_MOUSE.H10MO.D,Collection_1_m10_EGR1_MOUSE.H10MO.A,Collection_1_m11_EGR2_MOUSE.H10MO.C
	cluster_2	Collection_1_m21_HINFP_MOUSE.H10MO.C,Collection_1_m18_FLI1_MOUSE.H10MO.A,Collection_1_m20_GABPA_MOUSE.H10MO.A,Collection_1_m17_ETS2_MOUSE.H10MO.C,Collection_1_m19_GABP1_MOUSE.H10MO.C,Collection_1_m12_ELF1_MOUSE.H10MO.B,Collection_1_m13_ELK1_MOUSE.H10MO.B,
	cluster_3	Collection_1_m4_E2F2_MOUSE.H10MO.B,Collection_1_m5_E2F3_MOUSE.H10MO.B,Collection_1_m7_E2F5_MOUSE.H10MO.B,Collection_1_m9_E2F7_MOUSE.H10MO.D,Collection_1_m29_TFDP1_MOUSE.H10MO.D,Collection_1_m3_E2F1_MOUSE.H10MO.A,Collection_1_m6_E2F4_MOUSE.H10MO.C,Collecti
	cluster_4	Collection_1_m1_AHR_MOUSE.H10MO.B,Collection_1_m24_NRF1_MOUSE.H10MO.A
	cluster_5	Collection_1_m2_AP2D_MOUSE.H10MO.D,Collection_1_m31_ZFX_MOUSE.H10MO.C
	cluster_6	Collection_1_m28_SP4_MOUSE.H10MO.D
	cluster_7	Collection_1_m25_PAX5_MOUSE.H10MO.S
	cluster_8	Collection_1_m26_RFX1_MOUSE.H10MO.C

Heatmap cluster 2

RSAT matrix-clustering	cluster_1	Collection_1_m27_PLAG1_MOUSE.H10MO.S,Collection_1_m20_KLF6_MOUSE.H10MO.D,Collection_1_m31_SP1_MOUSE.H10MO.S,Collection_1_m7_EGR4_MOUSE.H10MO.D,Collection_1_m10_GLI2_MOUSE.H10MO.B,Collection_1_m11_GLI3_MOUSE.H10MO.B,Collection_1_m9_GLI1_MOUSE.H10MO.C,Col le
	cluster_2	Collection_1_m16_KLF15_MOUSE.H10MO.D,Collection_1_m28_PURA_MOUSE.H10MO.D,Collection_1_m22_MAZ_MOUSE.H10MO.D,Collection_1_m39_ZN148_MOUSE.H10MO.D,Collection_1_m30_SP1_MOUSE.H10MO.A,Collection_1_m32_SP3_MOUSE.H10MO.B
	cluster_3	Collection_1_m4_COE1_MOUSE.H10MO.C,Collection_1_m15_INSM1_MOUSE.H10MO.C,Collection_1_m1_AP2A_MOUSE.H10MO.A,Collection_1_m2_AP2B_MOUSE.H10MO.B
	cluster_4	Collection_1_m14_IKZF1_MOUSE.H10MO.C,Collection_1_m25_NR0B1_MOUSE.H10MO.D,Collection_1_m3_ARNT2_MOUSE.H10MO.D
	cluster_5	Collection_1_m21_KLF8_MOUSE.H10MO.C,Collection_1_m6_EGR3_MOUSE.H10MO.D
	cluster_6	Collection_1_m24_NFIA_MOUSE.H10MO.S,Collection_1_m34_YBOX1_MOUSE.H10MO.D
	cluster_7	Collection_1_m13_HIC1_MOUSE.H10MO.C
	cluster_8	Collection_1_m26_PLAG1_MOUSE.H10MO.D
	cluster_9	Collection_1_m33_SRBP2_MOUSE.H10MO.B
	cluster_10	Collection_1_m29_RREB1_MOUSE.H10MO.D
	cluster_11	Collection_1_m23_NFIA_MOUSE.H10MO.C
	cluster_12	Collection_1_m5_CTCF_MOUSE.H10MO.A
	cluster_13	Collection_1_m38_ZN143_MOUSE.H10MO.D
	cluster_14	Collection_1_m8_GCM1_MOUSE.H10MO.D

Heatmap cluster 3

RSAT matrix-clustering	cluster_1	Collection_1_m33_NFYA_MOUSE.H10MO.D,Collection_1_m50_PKNX1_MOUSE.H10MO.D,Collection_1_m3_CEBPZ_MOUSE.H10MO.D,Collection_1_m10_FOS_MOUSE.H10MO.A,Collection_1_m11_FOXI1_MOUSE.H10MO.B,Collection_1_m48_PBX3_MOUSE.H10MO.A,Collection_1_m36_NFYC_MOUSE.H10MO.B,Co
	cluster_2	Collection_1_m83_ZEP2_MOUSE.H10MO.D,Collection_1_m82_ZEP1_MOUSE.H10MO.D,Collection_1_m32_NFKB1_MOUSE.H10MO.B,Collection_1_m72_TF65_MOUSE.H10MO.S,Collection_1_m53_RELB_MOUSE.H10MO.C,Collection_1_m54_REL_MOUSE.H10MO.C,Collection_1_m30_NFAC1_MOUSE.H10MO.S,Co
	cluster_3	Collection_1_m16_HSF1_MOUSE.H10MO.A,Collection_1_m17_HSF2_MOUSE.H10MO.A
	cluster_4	Collection_1_m22_IRF5_MOUSE.H10MO.D,Collection_1_m21_IRF4_MOUSE.H10MO.C,Collection_1_m20_IRF3_MOUSE.H10MO.C,Collection_1_m66_STAT1_MOUSE.H10MO.A,Collection_1_m23_IRF7_MOUSE.H10MO.C,Collection_1_m18_IRF1_MOUSE.H10MO.C,Collection_1_m25_IRF9_MOUSE.H10MO.C,Co
	cluster_5	Collection_1_m59_SMAD1_MOUSE.H10MO.D,Collection_1_m79_UBIP1_MOUSE.H10MO.D,Collection_1_m13_HAND1_MOUSE.H10MO.D,Collection_1_m60_SMAD2_MOUSE.H10MO.D,Collection_1_m61_SMAD3_MOUSE.H10MO.C,Collection_1_m62_SMAD4_MOUSE.H10MO.C
	cluster_6	Collection_1_m80_ZBT18_MOUSE.H10MO.D,Collection_1_m2_ATOH1_MOUSE.H10MO.C,Collection_1_m74_TFE2_MOUSE.H10MO.S
	cluster_7	Collection_1_m58_RUNX3_MOUSE.H10MO.B,Collection_1_m49_PEBB_MOUSE.H10MO.C,Collection_1_m57_RUNX2_MOUSE.H10MO.B
	cluster_8	Collection_1_m64_SPIB_MOUSE.H10MO.B,Collection_1_m4_EHF_MOUSE.H10MO.A,Collection_1_m6_ELF3_MOUSE.H10MO.D,Collection_1_m8_ETV4_MOUSE.H10MO.B,Collection_1_m5_ELF2_MOUSE.H10MO.C,Collection_1_m68_STAT3_MOUSE.H10MO.B,Collection_1_m7_ELK3_MOUSE.H10MO.D,Collecti
	cluster_9	Collection_1_m42_P63_MOUSE.H10MO.D,Collection_1_m43_P73_MOUSE.H10MO.D
	cluster_10	Collection_1_m39_NKX32_MOUSE.H10MO.C,Collection_1_m37_NKX21_MOUSE.H10MO.D,Collection_1_m38_NKX28_MOUSE.H10MO.C
	cluster_11	Collection_1_m46_PAX6_MOUSE.H10MO.D,Collection_1_m47_PAX8_MOUSE.H10MO.D,Collection_1_m44_PAX2_MOUSE.H10MO.D,Collection_1_m45_PAX5_MOUSE.H10MO.D
	cluster_12	Collection_1_m41_P53_MOUSE.H10MO.C
	cluster_13	Collection_1_m71_TF2L1_MOUSE.H10MO.C
	cluster_14	Collection_1_m40_OLIG2_MOUSE.H10MO.B
	cluster_15	Collection_1_m52_PTF1A_MOUSE.H10MO.C
	cluster_16	Collection_1_m76_TLX1_MOUSE.H10MO.D,Collection_1_m77_TLX1_MOUSE.H10MO.S
	cluster_17	Collection_1_m15_HLTF_MOUSE.H10MO.D
	cluster_18	Collection_1_m26_KAISO_MOUSE.H10MO.B
	cluster_19	Collection_1_m73_TFCP2_MOUSE.H10MO.D
	cluster_20	Collection_1_m78_TYY1_MOUSE.H10MO.A
	cluster_21	Collection_1_m27_MAFA_MOUSE.H10MO.D
	cluster_22	Collection_1_m55_REST_MOUSE.H10MO.A
	cluster_23	Collection_1_m69_TBX20_MOUSE.H10MO.C
	cluster_24	Collection_1_m75_TGIF1_MOUSE.H10MO.D
	cluster_25	Collection_1_m12_FUBP1_MOUSE.H10MO.D
	cluster_26	Collection_1_m14_HEN1_MOUSE.H10MO.C
	cluster_27	Collection_1_m70_TEAD1_MOUSE.H10MO.D
	cluster_28	Collection_1_m29_MYB_MOUSE.H10MO.C
	cluster_29	Collection_1_m63_SOX4_MOUSE.H10MO.C
	cluster_30	Collection_1_m1_AP2C_MOUSE.H10MO.A
	cluster_31	Collection_1_m84_ZN423_MOUSE.H10MO.D
	cluster_32	Collection_1_m56_RFX2_MOUSE.H10MO.C
	cluster_33	Collection_1_m65_SPZ1_MOUSE.H10MO.D
	cluster_34	Collection_1_m81_ZBTB6_MOUSE.H10MO.D
	cluster_35	Collection_1_m28_MCR_MOUSE.H10MO.D

Heatmap cluster 4

RSAT matrix-clustering	cluster_1	Collection_1_m14_MYOD1_MOUSE.H10MO.C,Collection_1_m15_MYOG_MOUSE.H10MO.C,Collection_1_m8_HTF4_MOUSE.H10MO.C,Collection_1_m21_TBX5_MOUSE.H10MO.D,Collection_1_m10_MITF_MOUSE.H10MO.C,Collection_1_m22_TWST1_MOUSE.H10MO.D,Collection_1_m9_ITF2_MOUSE.H10MO.B,Col
	cluster_2	Collection_1_m5_E4F1_MOUSE.H10MO.D,Collection_1_m3_CREM_MOUSE.H10MO.C,Collection_1_m1_ATF1_MOUSE.H10MO.B,Collection_1_m2_CREB1_MOUSE.H10MO.B
	cluster_3	Collection_1_m19_SRBP1_MOUSE.H10MO.B
	cluster_4	Collection_1_m16_PAX2_MOUSE.H10MO.S
	cluster_5	Collection_1_m11_MLXPL_MOUSE.H10MO.D
	cluster_6	Collection_1_m7_HESX1_MOUSE.H10MO.D
	cluster_7	Collection_1_m6_EPAS1_MOUSE.H10MO.D
	cluster_8	Collection_1_m20_SUH_MOUSE.H10MO.C
	cluster_9	Collection_1_m4_CXXC1_MOUSE.H10MO.D
	cluster_10	Collection_1_m12_MTF1_MOUSE.H10MO.C
	cluster_11	Collection_1_m23_ZBT7A_MOUSE.H10MO.D

Heatmap cluster 5

RSAT matrix-clustering	cluster_1	Collection_1_m17_XBP1_MOUSE.H10MO.C,Collection_1_m11_MYC_MOUSE.H10MO.A,Collection_1_m8_MAX_MOUSE.H10MO.A,Collection_1_m10_MYCN_MOUSE.H10MO.B,Collection_1_m1_ARNT_MOUSE.H10MO.B,Collection_1_m2_BHE40_MOUSE.H10MO.B,Collection_1_m14_TFEB_MOUSE.H10MO.C,Collect
	cluster_2	Collection_1_m12_TFE2_MOUSE.H10MO.A

Heatmap cluster 6

RSAT matrix-clustering	cluster_1	Collection_1_m18_SOX5_MOUSE.H10MO.C,Collection_1_m19_SRY_MOUSE.H10MO.B,Collection_1_m12_FOXM1_MOUSE.H10MO.D,Collection_1_m10_FOXJ3_MOUSE.H10MO.A,Collection_1_m11_FOXJ3_MOUSE.H10MO.S,Collection_1_m4_FOXC1_MOUSE.H10MO.C,Collection_1_m5_FOXD1_MOUSE.H10MO.D,C

Heatmap cluster 7

RSAT matrix-clustering	cluster_1	Collection_1_m24_MAFK_MOUSE.H10MO.A,Collection_1_m20_JUN_MOUSE.H10MO.A,Collection_1_m48_SMRC1_MOUSE.H10MO.B,Collection_1_m12_FOSL1_MOUSE.H10MO.C,Collection_1_m19_JUND_MOUSE.H10MO.A,Collection_1_m13_FOSL2_MOUSE.H10MO.A,Collection_1_m11_FOSB_MOUSE.H10MO.C,C
	cluster_2	Collection_1_m15_GCR_MOUSE.H10MO.S,Collection_1_m45_PRGR_MOUSE.H10MO.S,Collection_1_m44_PRGR_MOUSE.H10MO.C,Collection_1_m14_GCR_MOUSE.H10MO.C,Collection_1_m2_ANDR_MOUSE.H10MO.B
	cluster_3	Collection_1_m10_FEV_MOUSE.H10MO.C,Collection_1_m9_ELF5_MOUSE.H10MO.D,Collection_1_m34_NFAC1_MOUSE.H10MO.A,Collection_1_m37_NFAC4_MOUSE.H10MO.C,Collection_1_m35_NFAC2_MOUSE.H10MO.B,Collection_1_m36_NFAC3_MOUSE.H10MO.B
	cluster_4	Collection_1_m28_MEIS2_MOUSE.H10MO.B,Collection_1_m17_HXA9_MOUSE.H10MO.D,Collection_1_m27_MEIS1_MOUSE.H10MO.C
	cluster_5	Collection_1_m51_SOX18_MOUSE.H10MO.D,Collection_1_m49_SOX10_MOUSE.H10MO.D,Collection_1_m21_LEF1_MOUSE.H10MO.C,Collection_1_m50_SOX15_MOUSE.H10MO.D,Collection_1_m52_SOX3_MOUSE.H10MO.C,Collection_1_m53_SOX9_MOUSE.H10MO.B,Collection_1_m64_TCF7_MOUSE.H10MO.C,
	cluster_6	Collection_1_m59_STAT6_MOUSE.H10MO.C,Collection_1_m6_BCL6_MOUSE.H10MO.C,Collection_1_m58_STAT4_MOUSE.H10MO.A,Collection_1_m56_STA5A_MOUSE.H10MO.A,Collection_1_m57_STA5B_MOUSE.H10MO.C
	cluster_7	Collection_1_m31_NDF1_MOUSE.H10MO.C,Collection_1_m61_TAL1_MOUSE.H10MO.S
	cluster_8	Collection_1_m62_TBX2_MOUSE.H10MO.D,Collection_1_m63_TBX3_MOUSE.H10MO.D,Collection_1_m7_BRAC_MOUSE.H10MO.D
	cluster_9	Collection_1_m29_MYBB_MOUSE.H10MO.D,Collection_1_m8_BRCA1_MOUSE.H10MO.D
	cluster_10	Collection_1_m16_GFI1B_MOUSE.H10MO.C
	cluster_11	Collection_1_m47_RUNX1_MOUSE.H10MO.B
	cluster_12	Collection_1_m39_NFKB2_MOUSE.H10MO.D
	cluster_13	Collection_1_m1_AIRE_MOUSE.H10MO.C
	cluster_14	Collection_1_m46_RFX3_MOUSE.H10MO.B
	cluster_15	Collection_1_m30_NANOG_MOUSE.H10MO.S
	cluster_16	Collection_1_m42_OVOL1_MOUSE.H10MO.C
	cluster_17	Collection_1_m55_SRF_MOUSE.H10MO.A
	cluster_18	Collection_1_m60_TAL1_MOUSE.H10MO.A
	cluster_19	Collection_1_m40_NKX22_MOUSE.H10MO.D
	cluster_20	Collection_1_m41_NR2E3_MOUSE.H10MO.C
	cluster_21	Collection_1_m54_SP11_MOUSE.H10MO.A
	cluster_22	Collection_1_m66_TF65_MOUSE.H10MO.C
	cluster_23	Collection_1_m65_TEAD3_MOUSE.H10MO.D
	cluster_24	Collection_1_m43_PRD14_MOUSE.H10MO.D

Heatmap cluster 8

RSAT matrix-clustering	cluster_1	Collection_1_m7_DDIT3_MOUSE.H10MO.C,Collection_1_m9_NFIL3_MOUSE.H10MO.C,Collection_1_m4_CEBPE_MOUSE.H10MO.A,Collection_1_m5_CEBPG_MOUSE.H10MO.C,Collection_1_m8_HLF_MOUSE.H10MO.C,Collection_1_m6_DBP_MOUSE.H10MO.B,Collection_1_m3_CEBPD_MOUSE.H10MO.B,Collect

Heatmap cluster 9

RSAT matrix-clustering	cluster_1	Collection_1_m11_CRX_MOUSE.H10MO.A,Collection_1_m63_OTX2_MOUSE.H10MO.C,Collection_1_m77_PRRX1_MOUSE.H10MO.D,Collection_1_m68_PITX2_MOUSE.H10MO.D,Collection_1_m12_CRX_MOUSE.H10MO.S,Collection_1_m62_OTX1_MOUSE.H10MO.D,Collection_1_m16_EVI1_MOUSE.H10MO.B,Col
	cluster_2	Collection_1_m71_PO3F1_MOUSE.H10MO.C,Collection_1_m57_NANOG_MOUSE.H10MO.A,Collection_1_m74_PO5F1_MOUSE.H10MO.A,Collection_1_m81_SOX2_MOUSE.H10MO.A,Collection_1_m67_PIT1_MOUSE.H10MO.C,Collection_1_m69_PO2F1_MOUSE.H10MO.B,Collection_1_m70_PO2F2_MOUSE.H10MO.
	cluster_3	Collection_1_m33_HNF6_MOUSE.H10MO.C,Collection_1_m61_ONEC2_MOUSE.H10MO.D,Collection_1_m18_EVX2_MOUSE.H10MO.C,Collection_1_m43_HXC6_MOUSE.H10MO.D,Collection_1_m10_CDX4_MOUSE.H10MO.A,Collection_1_m17_EVX1_MOUSE.H10MO.C,Collection_1_m8_CDX1_MOUSE.H10MO.C,Col
	cluster_4	Collection_1_m83_TEAD4_MOUSE.H10MO.D,Collection_1_m82_TBP_MOUSE.H10MO.C,Collection_1_m52_MEF2A_MOUSE.H10MO.B,Collection_1_m53_MEF2C_MOUSE.H10MO.B,Collection_1_m54_MEF2D_MOUSE.H10MO.C
	cluster_5	Collection_1_m3_ARI3A_MOUSE.H10MO.S,Collection_1_m49_ISL1_MOUSE.H10MO.D,Collection_1_m29_HMGA1_MOUSE.H10MO.D,Collection_1_m15_DLX3_MOUSE.H10MO.C,Collection_1_m60_NOBOX_MOUSE.H10MO.C,Collection_1_m66_PDX1_MOUSE.H10MO.C,Collection_1_m78_PRRX2_MOUSE.H10MO.C,
	cluster_6	Collection_1_m2_ARI3A_MOUSE.H10MO.D,Collection_1_m56_MSX3_MOUSE.H10MO.D
	cluster_7	Collection_1_m20_FOXP3_MOUSE.H10MO.D
	cluster_8	Collection_1_m45_HXD10_MOUSE.H10MO.D
	cluster_9	Collection_1_m27_GFI1_MOUSE.H10MO.C
	cluster_10	Collection_1_m7_CDC5L_MOUSE.H10MO.D,Collection_1_m84_TEF_MOUSE.H10MO.D
	cluster_11	Collection_1_m28_HBP1_MOUSE.H10MO.D
	cluster_12	Collection_1_m19_FOXC2_MOUSE.H10MO.D,Collection_1_m79_SOX13_MOUSE.H10MO.D
	cluster_13	Collection_1_m30_HMGA2_MOUSE.H10MO.D
	cluster_14	Collection_1_m80_SOX17_MOUSE.H10MO.D
	cluster_15	Collection_1_m46_HXD13_MOUSE.H10MO.D
	cluster_16	Collection_1_m4_ARI5B_MOUSE.H10MO.C
	cluster_17	Collection_1_m38_HXA7_MOUSE.H10MO.D
	cluster_18	Collection_1_m6_BATF_MOUSE.H10MO.B
	cluster_19	Collection_1_m58_NKX25_MOUSE.H10MO.C

Heatmap cluster 10

RSAT matrix-clustering	cluster_1	Collection_1_m2_COT1_MOUSE.H10MO.S,Collection_1_m9_NR2C1_MOUSE.H10MO.C,Collection_1_m16_RARB_MOUSE.H10MO.D,Collection_1_m6_ESR2_MOUSE.H10MO.S,Collection_1_m7_NR1I2_MOUSE.H10MO.S,Collection_1_m8_NR1I3_MOUSE.H10MO.S,Collection_1_m20_VDR_MOUSE.H10MO.S,Collection_1_m17_RARG_MOUSE.H10MO.S,Collection_1_m13_PPARA_MOUSE.H10MO.S,Collection_1_m15_RARA_MOUSE.H10MO.S,Collection_1_m18_RXRB_MOUSE.H10MO.C,Collection_1_m19_THA_MOUSE.H10MO.S,Collection_1_m4_ERR1_MOUSE.H10MO.A,Collection_1_m5_ERR2_MOUSE.H10MO.B,Collection_1_m14_PPARG_MOUSE.H10MO.S,Collection_1_m1_COT1_MOUSE.H10MO.B,Collection_1_m10_NR4A1_MOUSE.H10MO.C,Collection_1_m11_NR4A2_MOUSE.H10MO.C,Collection_1_m12_NR4A3_MOUSE.H10MO.D,Collection_1_m3_COT2_MOUSE.H10MO.B

Heatmap cluster 11

RSAT matrix-clustering	cluster_1	Collection_1_m18_PPARG_MOUSE.H10MO.A,Collection_1_m5_HNF4A_MOUSE.H10MO.A,Collection_1_m6_HNF4G_MOUSE.H10MO.C,Collection_1_m1_COT2_MOUSE.H10MO.S,Collection_1_m17_PPARD_MOUSE.H10MO.D,Collection_1_m12_NR2C2_MOUSE.H10MO.A,Collection_1_m16_PPARA_MOUSE.H10MO.C,
	cluster_2	Collection_1_m14_NR5A2_MOUSE.H10MO.A,Collection_1_m25_STF1_MOUSE.H10MO.B,Collection_1_m2_ERR3_MOUSE.H10MO.B,Collection_1_m15_NR6A1_MOUSE.H10MO.B,Collection_1_m24_RXRG_MOUSE.H10MO.C
	cluster_3	Collection_1_m10_NR1I2_MOUSE.H10MO.C,Collection_1_m11_NR1I3_MOUSE.H10MO.C,Collection_1_m26_THA_MOUSE.H10MO.C,Collection_1_m27_THB_MOUSE.H10MO.C
	cluster_4	Collection_1_m28_THB_MOUSE.H10MO.S,Collection_1_m21_RORA_MOUSE.H10MO.B,Collection_1_m22_RORG_MOUSE.H10MO.C
	cluster_5	Collection_1_m29_VDR_MOUSE.H10MO.C,Collection_1_m3_ESR1_MOUSE.H10MO.B,Collection_1_m4_ESR2_MOUSE.H10MO.B
	cluster_6	Collection_1_m19_RARA_MOUSE.H10MO.C,Collection_1_m20_RARG_MOUSE.H10MO.C
	cluster_7	Collection_1_m23_RXRA_MOUSE.H10MO.C,Collection_1_m7_NR1D1_MOUSE.H10MO.D
	cluster_8	Collection_1_m9_NR1H4_MOUSE.H10MO.C

Table S1. Full list of REs from clusters 1 to 11